Deep-Sea Research Part II 162 (2019) 164–179

Contents lists available at ScienceDirect

Deep-Sea Research Part II

journal homepage: www.elsevier.com/locate/dsr2

A video seafloor survey of epibenthic communities in the Pacific Arctic including Distributed Biological Observatory stations in the northern Bering and Chukchi seas

Lee W. Cooper[a,*], Marisa L. Guarinello[b], Jacqueline M. Grebmeier[a], Alynne Bayard[a], James R. Lovvorn[c], Christopher A. North[d], Jason M. Kolts[e]

[a] Chesapeake Biological Laboratory, University of Maryland Center for Environmental Science, Solomons MD, 20688, USA
[b] INSPIRE Environmental, 88 Silva Ln, Newport, RI, 02840, USA
[c] Department of Zoology, Southern Illinois University, Carbondale, IL, 62901, USA
[d] Department of Botany, University of Wyoming, Laramie, WY 82071, USA
[e] Department of Biology, Metropolitan University of Denver, Denver, CO, 80217-3362, USA

ARTICLE INFO

Keywords:
Bering sea
Chukchi sea
Epibenthos
Video imagery
Distributed Biological Observatory

ABSTRACT

Two separate efforts to characterize epibenthic communities in the northern Bering and Chukchi seas using video imagery from a drop camera system have now been completed. In the initial phase in 2008, we acquired video imagery from the USCGC *Healy* while drifting on station during the multidisciplinary Bering Sea Program and used cluster analysis and non-metric multidimensional scaling to identify epibenthic assemblage types and associated sediment characteristics based upon along-track epifaunal counts. We also quantified the areal density of easily recognizable organisms such as brittle stars (*Ophiura* sp.) and sea stars, which were abundant and easily identified. While sampling was not extensive enough to rigorously compare the density of epifauna with trawling data available from prior years, our observations confirmed the characteristics of epifaunal communities sampled through much more labor-intensive trawling. Densities of epifauna that could be readily enumerated were of the same order of magnitude in both types of observations. During the second phase in 2016 and 2017 of video observations from the CCGS *Sir Wilfrid Laurier*, we improved the quality of imagery, and obtained seafloor video footage from each station in the internationally coordinated sampling grid in the Distributed Biological Observatory (DBO). This grid lies in the productive waters of the northern Bering and Chukchi seas. Quantitative analysis was not undertaken in this second phase, but the imagery confirms the presence of specific organismal community assemblages that can be related to environmental factors such as sediment grain size and water mass identity that are available from other project data collected during the Bering Sea and DBO projects. For example, sandier sediments typically had diverse epifaunal communities including filter feeders as significant community components. In muddier sediments, deposit feeders such as brittle stars predominated. All the second phase video footage has been posted in both abbreviated form on the video-sharing website youtube.com, and longer (10 min per station) versions are freely downloadable from a Google Drive server. Future videography may help identify changes in epibenthic diversity and community composition and could be successfully evaluated with crowd-sourced citizen science and/or more traditional scientific documentation.

1. Introduction

The community structure and abundance of benthic infauna is now well known for much of the Pacific Arctic region, based upon extensive surveys over the past several decades, (e.g. Grebmeier, 2012; Grebmeier and Cooper, 2016b, 2015). However, it is more time-consuming and challenging to sample the epibenthos, as trawling is normally required and some areas with rocky, hard bottoms cannot be sampled effectively. Despite these limitations, trawling has been undertaken in many areas of the Pacific Arctic and provides baseline information on this important component of the benthic biological community, (e.g. Bluhm et al., 2009; Feder et al., 2005; Ravelo et al.,

* Corresponding author. .
E-mail address: cooper@umces.edu (L.W. Cooper).

https://doi.org/10.1016/j.dsr2.2019.05.003
Received 25 September 2018; Received in revised form 1 May 2019; Accepted 2 May 2019
Available online 04 May 2019

2014; Lovvorn et al., 2018).

The establishment in 2010 of a long-term observing scheme through the Distributed Biological Observatory (DBO) in the northern Bering and Chukchi seas (Moore and Grebmeier, 2018) provides the opportunity for change detection in epibenthic communities. Video observations of the seafloor are one potential method for assessing changes on a year-to-year basis in the presence and abundance of epibenthic organisms at specific locations (Glover et al., 2010; Kortsch et al., 2012), such as in the DBO station grid that is sampled annually. Complexities and limitations must be considered in the interpretation of video imagery that attempts to quantify and characterize marine communities. These topics have been discussed in many reviews including recent contributions from Rattray et al. (2014) and Romero-Ramirez et al. (2016). Iken et al. (2018) have provided some specific guidance on representative epifaunal sampling in the DBO and documented differences in epifaunal versus infaunal sampling requirements.

Here we report our experience in using a drop camera video system to identify and, where possible, quantify epibenthic communities in the Northern and Eastern Bering Sea shelf. Initially this work was undertaken in the spring of 2008, using the United States Coast Guard Cutter (USCGC) *Healy* during the Bering Sea Program supported by the North Pacific Research Board and the US National Science Foundation (Wiese et al., 2012; Lomas and Stabeno, 2014; Harvey and Sigler, 2013; Van Pelt et al., 2016). This video survey was intended in part as a proof of concept to demonstrate how epibenthic communities could be characterized when they were not otherwise well sampled by trawling. There was also an opportunity in these observations to compare epifaunal density and biomass with similar estimates from recent prior trawling surveys, so comparing estimates of epifaunal density and biomass for organisms that were easy to quantify (brittle stars and sea stars) was also incorporated into this study.

The second phase of this project was conducted in the context of the DBO program (Moore and Grebmeier, 2018) where the main goal is to rapidly make available data for evaluating possible changes in the ecosystem, rather than to explore ecological complexities in detail. The DBO project encourages coordinated sampling of specific locations in the Pacific Arctic that have been identified as having high productivity and/or biodiversity. Providing contemporary documentation of the epibenthic communities of the DBO from video imagery is therefore an appropriate goal of this effort. Given these objectives and taking advantage of the excellent station-keeping capabilities of the Canadian Coast Guard Ship (CCGS) *Sir Wilfrid Laurier*, we completed baseline seafloor videography for all the benthic stations occupied as part of DBO sampling in the northern Bering and Chukchi Seas, both in 2016 and 2017. As part of this report, we are making the video imagery freely available and providing qualitative annotations of the epibenthic communities observed. These data establish a reference condition against which results from ongoing epibenthic trawling in the Pacific Arctic region (e.g. Mueter et al., 2018) can be compared, creating the opportunity to document changes in the epibenthic communities of the northern Bering and Chukchi Seas. For example, future work might include re-filming of the DBO stations and use of crowd-sourced annotations, e.g. Zooniverse (https://www.zooniverse.org/), Amazon Mechanical Turk (https://www.mturk.com/) and other approaches that would be able to identify changes in epibenthic communities, (e.g. Durden et al., 2016; Gomes-Pereira et al., 2016), such as those already described for the infaunal communities of the DBO region (Grebmeier, 2012).

2. Methods

The drop camera system used was manufactured and assembled by A.G.O. Environmental Electronics Ltd. (Victoria, B.C., Canada). The system (Fig. 1) includes two positioning lasers for measuring distances recorded in the video images, an undersea video camera, a thermometer, and pressure transducer. Initially, video footage was monitored onboard and recorded onto a ship-based video camera. More recently recording has been directly to an Apple Mac-mini computer using a RCA to USB converter. Most deployments were by hand using a 200-m electronic cable. We also experimented with using shipboard winches, but found we had better control of the camera and its proximity to the seafloor with hand deployments. We also benefited from installation of a video monitor at the ship rail during deployment, so the person handling the cable could almost instantaneously pull the camera up or down if needed, depending upon sea state and ship motion. Typically, seafloor footage was obtained for 10 min at all benthic stations that were occupied during both the initial survey phase in 2008 (Fig. 2), as well as at all DBO stations occupied, repeating most occupations in 2017 that had been filmed in 2016 (Fig. 3).

2.1. Initial survey phase, 2008

In March to May 2008, we recorded digital video footage at a total of 47 shallow water stations (< 150 m depth) on *Healy* cruises 0801 (n = 9) and 0802 (n = 38) (Fig. 2). We transferred the images from these tapes to computer files and individually edited the imagery using Apple iMovie software to remove extraneous, non-useful footage. Footage was judged not useable because of sea-ice conditions interfering with deployment, poor seafloor visibility, winds causing rapid ship movement that could not be rectified by station keeping, or other operational problems. In some cases, due to a high speed of ship drift, video-processing transformations such as slowing the number of frames per second was necessary for viewing and analyzing the imagery.

In the 2008 video sampling, a total of 41 stations contained footage useable for analysis (Fig. 2). All 41 video clips were evaluated in their entirety for qualitative description of surface sediments and biological communities. In addition, we determined quantitative abundance data for selected organisms at 19 of these sites (all from HLY0802).

Where dominant epifauna, such as brittle stars, were observed with high frequency (e.g. every frame), each occurrence was not explicitly counted. Instead, in these videos where, for example, brittle stars were always observed, we categorized these species as “abundant” (1–3 brittle stars per frame) or “frequent” (> 3 brittle stars per frame). By contrast, the maximum sea star count was 246 in 10 min of filming. Therefore, the number of sea stars occurring at the most “abundant” sites was lower than the number of brittle stars occurring at “frequent” sites. We applied the former category (frequent) to those stations where multiple individual seastars occurred in every image frame and the latter (abundant) to those stations where only a few individuals (~1–3) appeared in individual frames and some lacked the fauna altogether. These data are semi-quantitative because each video recorded a different total seafloor area depending upon camera height above the seafloor, ship drift speed, and total recording time, but this imagery was used to characterize the biological assemblages.

We used still frame image analysis to quantify average abundance per square meter for dominant epifauna at all stations where it was practical. Video imagery with significant ship motion or low visibility (poor video quality) and/or the absence of brittle stars and sea stars, the most easily enumerated organisms, were the basis for determining stations that were not enumerated. Where enumeration was practical, we estimated the average abundance of dominant epifauna using still frame analysis (images captured every 10–20 s). We conducted this quantitative analysis at all seafloor sites in which brittle stars, *Ophiura* sp. (stations n = 10) and sea stars (various species; stations n = 3) were observed with high frequency during qualitative analysis. We also evaluated 6 additional stations using still frame analysis where there were no clearly dominant epifauna, so a total of 19 sites were evaluated in the initial portion of the study. These were stations where more than one species and discrete individuals were practical to enumerate. For still frame analysis, we used images sampled at equal intervals (every 10–20 s) in each video, resulting in 40 images per station. Two stations, NP1 and SL12, had relatively short video records (due to ship motion)

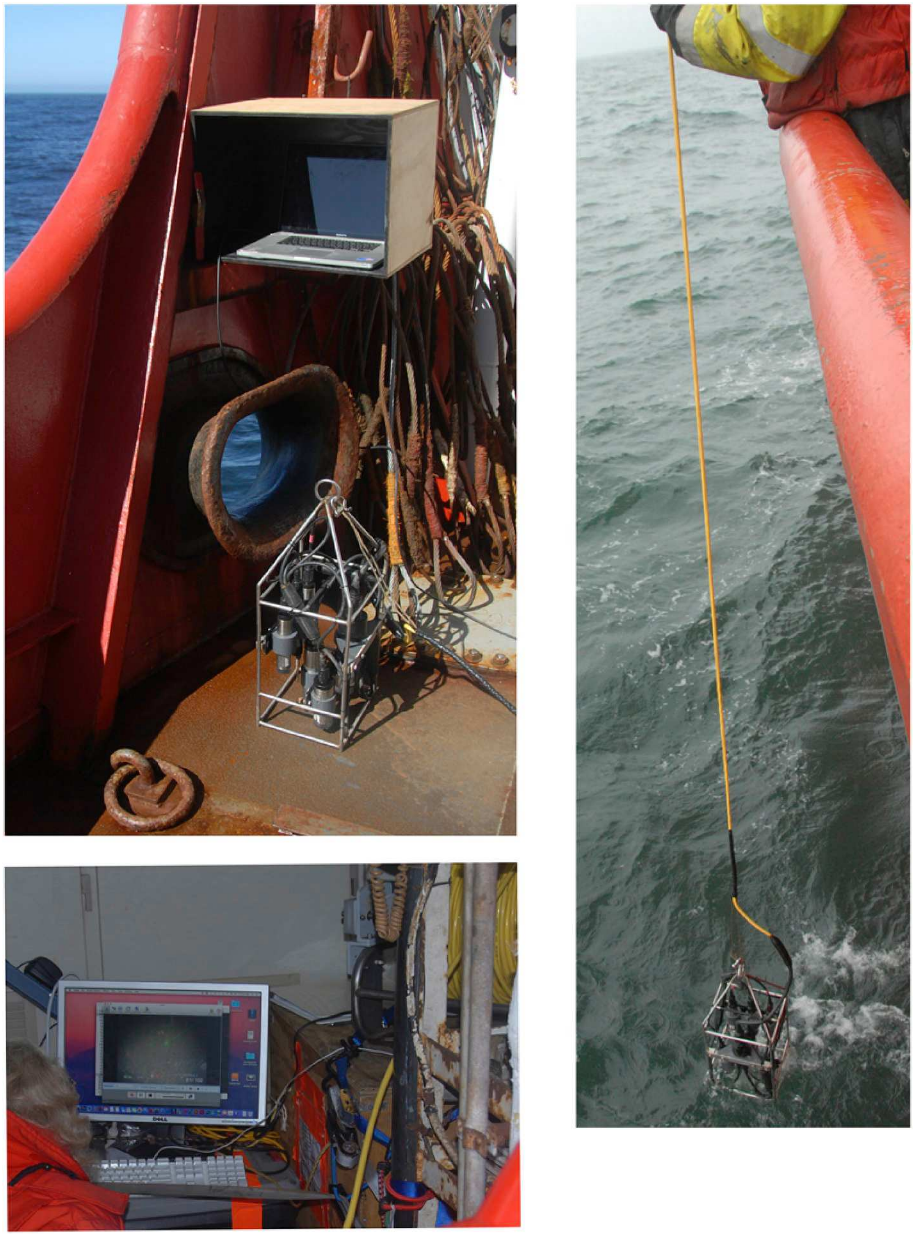

Fig. 1. Camera system on deck (upper left), including slave monitor (i.e. monitor networked to the computer used to control video recording); hand deployment (right) and video capture onto Mac Mini computer (lower left). 200-m cable and hand winch is visible to the right of Mac Mini computer.

and when sampled at intervals of 10 s resulted in fewer than the 40 still images assessed for all other stations (12 and 22 still frames, respectively). We used Adobe Photoshop software and the camera system positioning lasers to facilitate image analysis. Data recorded included: 1) area analyzed; 2) counts, percent cover, and density (numbers per m^2) of epifauna by family or species; 3) counts of infauna were made when visible, such as when bivalves present had body parts above the surface of the sediments; 4) the type of dominant and secondary sediments, which are based upon archived sediment grain data at the same stations (Grebmeier and Cooper, 2016a); 5) percent cover of each sediment type, again based upon archived grain size data (Grebmeier and Cooper, 2016a); 6) whether small-scale benthic topography was physical or biological in origin; and 7) measures of small-scale benthic topography including counts, distribution, density, minimum and maximum size of burrows, pits, mounds, and track lines.

We used similarity-based multivariate statistics in PRIMER v6 (Primer-E, Ltd., Plymouth, U.K.) to evaluate descriptive habitat groupings based on along-track epifaunal counts. Within the PRIMER software, we used cluster analysis (CLUSTER), non-metric multidimensional scaling (MDS), similarity percentage analysis (SIMPER), and multivariate analysis of variance (ANOSIM) on Bray-Curtis dissimilarity matrices of square-root transformed data. ANOSIM tested whether or not the sediment and assemblage types from qualitative analysis were distinguishable based on count data. The SIMPROF test was run with CLUSTER analysis to identify significant clusters of biological count data. We used SIMPER on square-root transformed data to characterize these groupings.

2.2. Comparisons with trawl data from 2007

Abundances of organisms that could be enumerated, primarily brittle stars in the 2008 video data, were compared with trawl abundance and biomass data collected the previous year, 2007. Trawl methods followed Cui et al. (2009). Briefly, samples were collected from 16 May to 18 June 2007 using a beam trawl (4.3 m long, 3.7 mm (1.5 in) stretched mesh, 4 m wide opening) that was deployed at 52

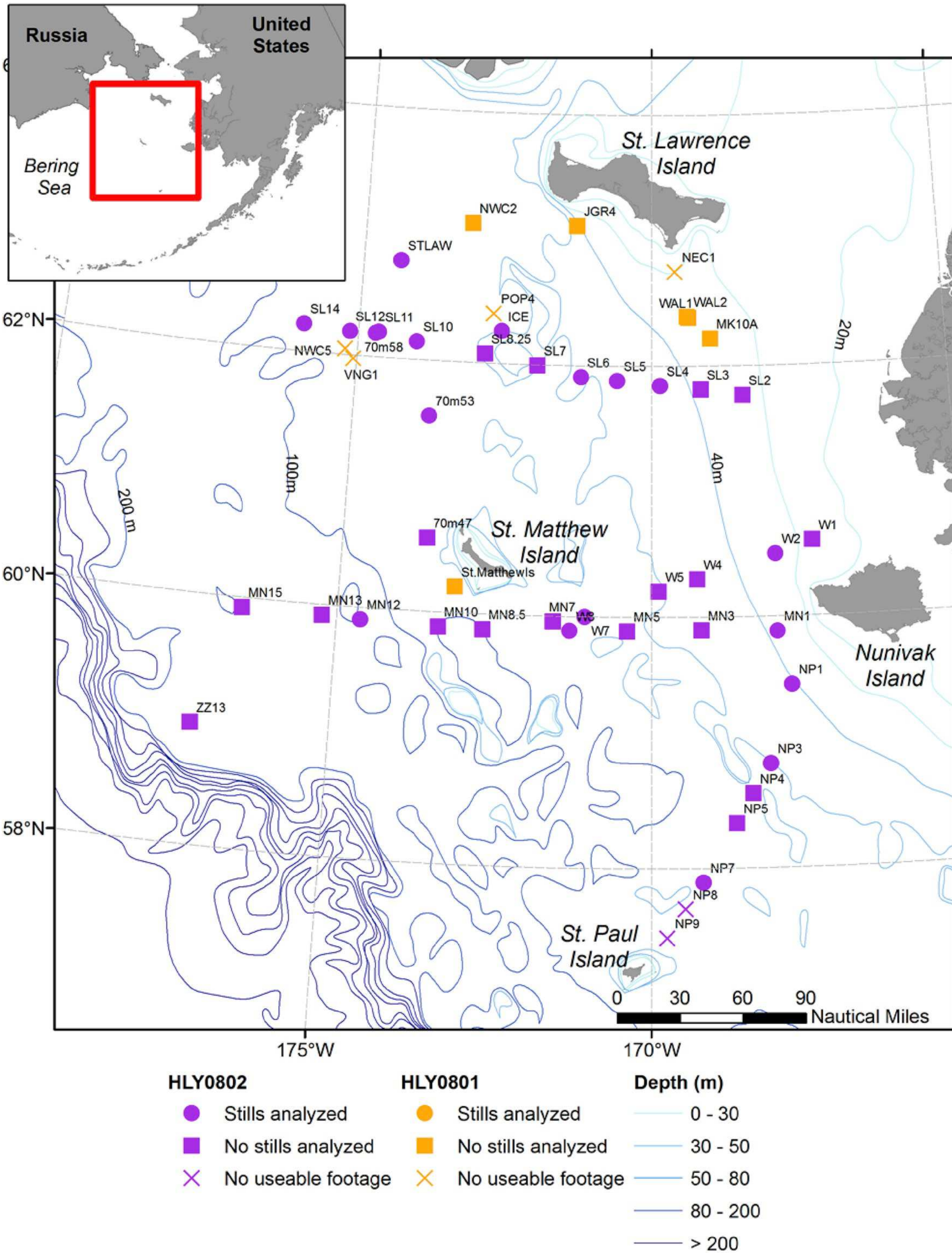

Fig. 2. Sites sampled using the underwater video camera systems during March (HLY0801) and May (HLY0802) 2008 Bering Sea Project cruises on the USCGC *Healy*. We excluded sites with no useable footage from qualitative and quantitative analysis. We performed qualitative habitat analysis on all other sites.

stations. All trawls were deployed at a speed of ~2 knots for durations on the bottom of 2–25 min. Abundance data for *Ophiura* spp. were generated as described in Cui et al. (2009), specifically using the area calculated to have been swept by the net. This was based upon distances towed on the bottom that were calculated for the beam trawl by means of shipboard GPS and a trawl-mounted depth logger (Sensus Ultra, ReefNet) that allowed us to determine the precise period the trawls were on the bottom.

2.3. DBO survey phase, 2016–2017

Similar methods as above were used for collecting 10-min video clips during the DBO cruises of the CCGS *Sir Wilfrid Laurier* (SWL) in July 2016 and July 2017, at each station in the DBO sampling grid. Water depths were less than 80 m, except for several stations in the Barrow Canyon undersea feature that were as deep as 135 m. We achieved higher quality imagery because active station keeping by the ship decreased resolution problems caused by drifting very quickly over

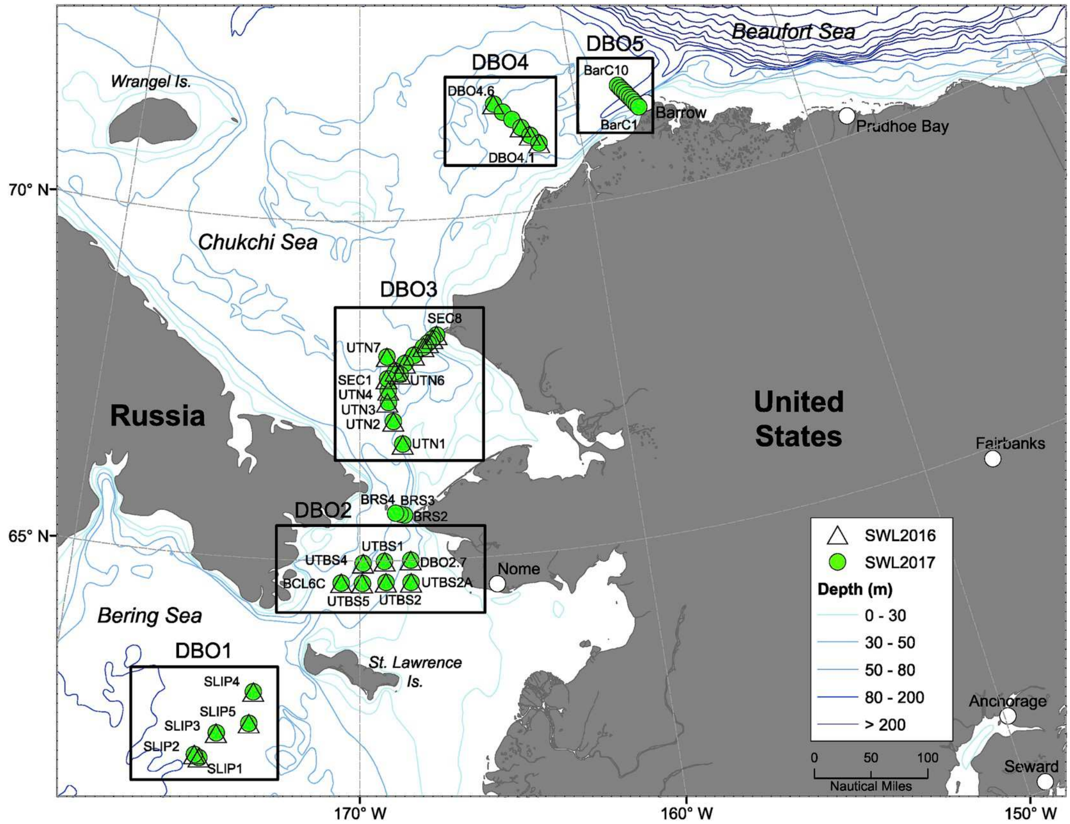

Fig. 3. Distribution of Distributed Biological Observatory (DBO) regions and associated stations in the northern Bering and Chukchi seas sampled during 2016 and 2017 from the CCGS *Sir Wilfrid Laurier* (SWL). Individual station names are given in each DBO bounding box.

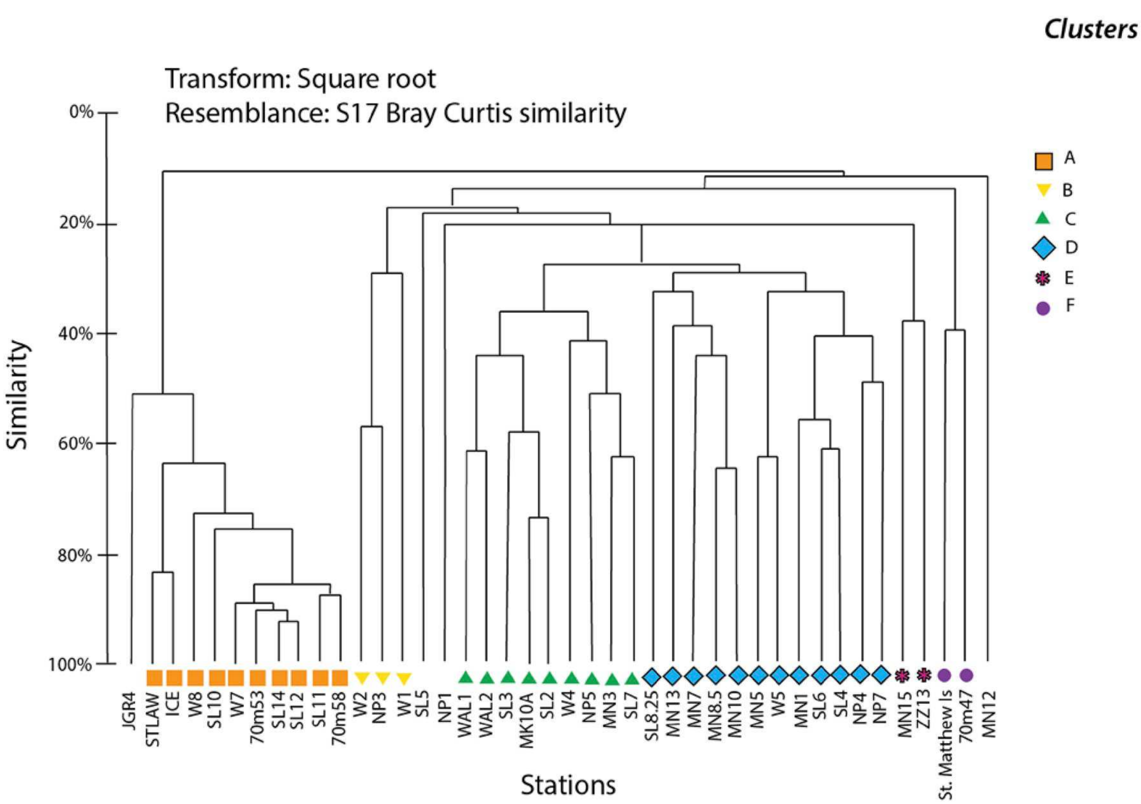

Fig. 4. Station cluster groupings (6) by percent similarity (vertical axis) for video imagery of epifaunal composition from USCGC *Healy* cruises 0801 and 0802 (see Fig. 2 for station locations). Individual station names are presented on the horizontal axis.

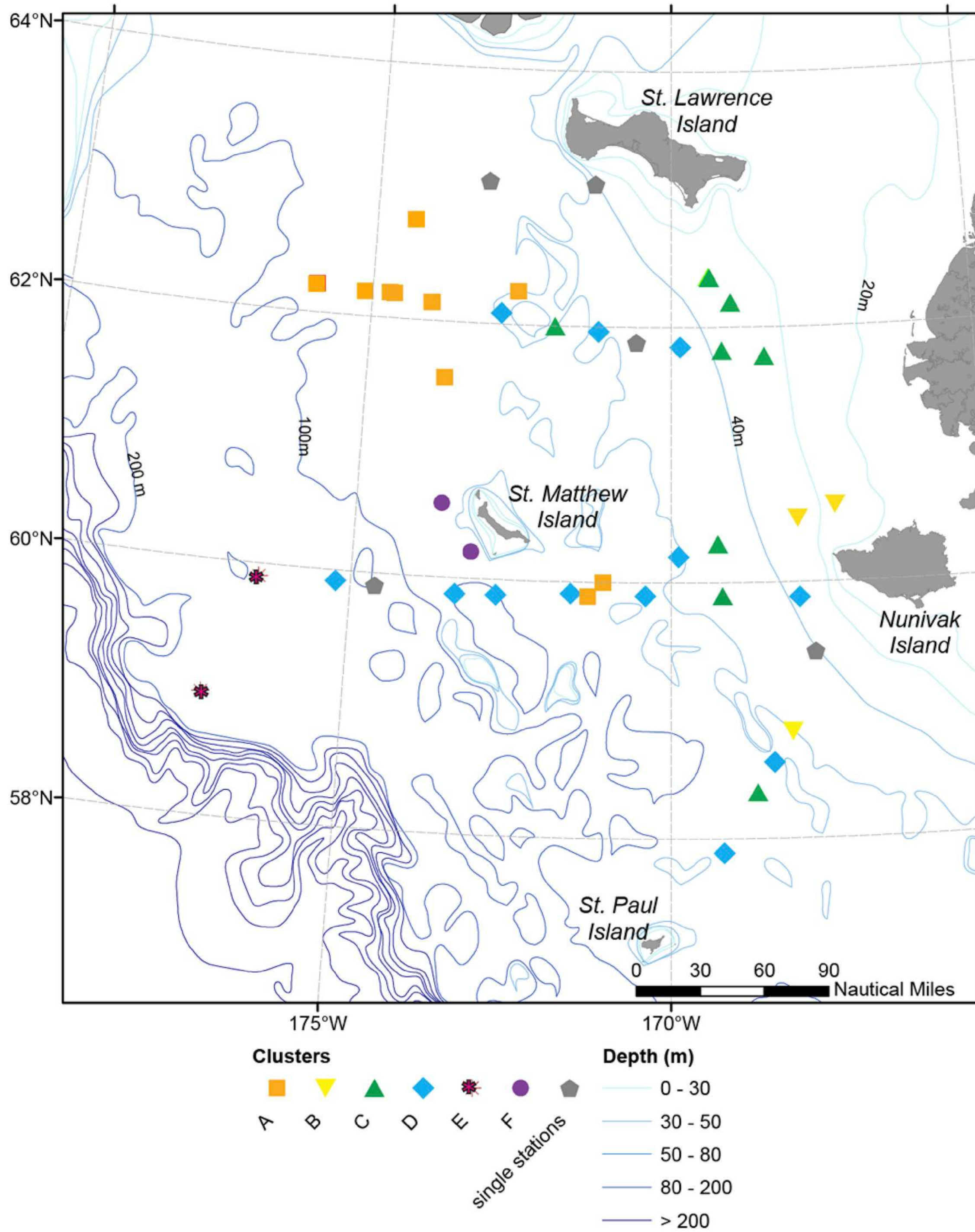

Fig. 5. Six epibenthic clusters of video-produced epibenthic abundance data from 2008. Cluster A represents brittle stars, primarily concentrated in the northern and western areas of the St. Lawrence Island Polynya (SLIP) area (DBO1 region).

the seafloor. The videos were edited into two formats, a short "highlight" tape that was posted for all stations on the video sharing site youtube.com and the full 10-min length tape for each station, which were uploaded as digital video files to the file storage service hosted by Google Drive.

For the SWL 2016 and 2017 epibenthic videos, we identified dominant (1–5 most common) epifauna from each station. We used statistical clustering via PRIMER software to define macrofaunal groupings, based upon prior taxonomic identifications undertaken in the laboratory with preserved specimens collected by van Veen grab in 2014 from the same stations (SWL2014). We used these groupings as the basis for qualitatively separating the major benthic groups observed in the epibenthic surveys for SWL16 and SWL17.

3. Results and discussion

3.1. Initial survey phase, 2008

The epibenthic assemblages (Fig. 4) represent significantly distinct groups of taxa based on ANOSIM results of abundance ($R = 0.527$, $p < 0.001$). Sediment types were also found to be significantly different ($R = 0.165$, $p < 0.017$), particularly if sediment grain size

Table 1
MDS clusters, with dominant species, and example images from HLY0802. The green laser points in the images are 10 cm apart. (Note: Temperature readings of 552 °C are spurious due to a problem with the sensor on the camera for this cruise).

Cluster A			
	% similarity	75.08	
	Dominant sp	brittle stars, Ophiura sp. (83.05% contribution to sim)	
	Stations	10: STLAW, SL10, SL11, SL12, SL14, W7, W8, ICE, 70m53, 70m58	
Cluster B			
	% similarity	38.33	
	Dominant sp	sea star, Asterias amurensis (100% contribution to sim)	
	Stations	3: W1, W2, NP3	
Cluster C			
	% similarity	42.28	
	Dominant sp	tanner crab, Chionoecetes sp. (34.93% contribution to sim)	
	Stations	9: WAL1, WAL2, MK10A, NP5, MN3, SL2, SL3, SL7, W4	
Cluster D			
	% similarity	34.27	
	Dominant sp	hermit crab, Pagurus sp. (41.82% contribution to sim)	
	Stations	12: NP4, NP7, MN1, MN5, MN7, MN8.5, MN10, MN13, SL4, SL6, SL8.25, W5	
Cluster E			
	% similarity	37.72	
	Dominant sp	bottom-feeding squid & fish (76.82% contribution to sim)	
	Stations	2: MN15, ZZ13	
Cluster F			
	% similarity	39.56	
	Dominant sp	sea star, Crossaster papposus (22.46% contribution to sim)	
	Stations	2: 70m47, St. Matthew Island	

distributions alone were considered (R = 0.193, $p < 0.008$) based upon data from Grebmeier and Cooper (2016a). Although only Cluster A was found to be significant using SIMPROF, we delineated 5 additional cluster groups from the CLUSTER analysis that show distinct patterns among mobile and sessile epifauna (Figs. 4 and 5). We also examined the biotic and abiotic descriptions of these clusters (Table 1) using MDS plots (Fig. 6), specifically how the clusters could be distinguished by sediment types and biological community assemblages. Cluster A was dominated by brittle stars, Cluster B and D by sea stars, and the remaining clusters by an assortment of mobile and sessile epifauna (Table 1).

The larger brittle stars could be reliably identified on the video as *Ophiura sarsi* and were generally found at lower densities than smaller specimens of *Ophiura* spp. (Table 2), which included some juvenile *Ophiura sarsi* in addition to other species that include *O. robusta*. For example, mean densities of *O. sarsi* ranged from less than 1 to over 180 per m^2 with a median of nearly 50 (mean = 53 ± 66 SD) compared to a range of 18 to nearly 600 with a median of 245 (mean = 290 ± 251 SD) for the smaller individuals that could not be identified to species (Table 2). Total brittle stars, regardless of species, were observed at about half of the sampled stations with a combined median, where observed, of 98 per m^2 (mean = 229 ± 224 SD; Fig. 7). *Ophiura* sp. densities calculated from a 2007 *Healy* epibenthic trawl survey (cruise HLY0702) were of the same order of magnitude as values determined by video analysis (Fig. 7). Sea star mean densities (Table 3) were much lower than those of brittle stars and ranged from 1.5 to nearly 8 per m^2 with median of 3.8 per m^2. No clear spatial patterns in density were detected in our analysis (Fig. 7). We used a conversion factor based on HLY0702 epibenthic trawl data (Lovvorn et al., 2018) to estimate wet weight biomass of brittle stars per unit area and a species-specific conversion factor (Stoker, 1978) to estimate carbon biomass of brittle stars per unit area (Fig. 8a and b). Both trawl and video data estimates of brittle star biomass range upwards of 200 g m^{-2} (Fig. 8a). Organic carbon biomass values from video data exceeded 4.0 g m^{-2} (Table 2), whereas the maximum estimate from trawl data was just above 1.6 g m^{-2} (Fig. 8b). The trawling took place one-to two years before the 2008 video tapes were obtained, and sampling locations, while in the same region south of Saint Lawrence Island, were not at identical locations. One of the other limitations for any comparison between the results from the trawling relative to the video surveys was that sea-ice coverage was much greater (in March 2008) during the video survey, which was also during a shorter cruise, and it was not practical to fully match the locations where trawls were undertaken in May-June 2007 under a retreating sea-ice regime. We therefore think it would be unwise to conclude that where the video analysis indicated higher wet mass of brittle stars than trawling (e.g. in the stations farthest to the southwest of Saint Lawrence Island), that the video surveys are inherently more accurate. One implication is that the trawls may be inefficient in collecting all epifauna that were visible in the video surveys, but any such conclusion was beyond the scope of the sampling that we were able accomplish. In the same potential comparison with organic carbon biomass per square meter (Fig. 8b), the area to the far southwest of Saint Lawrence Island on the other hand sometimes had higher organic biomass based upon the trawl data, which possibly reflects the low organic carbon content of brittle stars versus other epifauna (e.g. molluscs), so the biases of each epifaunal collection method probably also play a role. Overall, while the data collected from the video survey and the samples undertaken by trawling in 2007 agree to within an order of magnitude (Fig. 8a and b), further sampling would be required to fully reconcile the two data sets.

Mean densities and sizes of sediment microtopography features varied widely across stations dominated by brittle stars, sea stars, and by neither (Table 4). Burrows were found at all sites but pits were not found at sites dominated by sea stars, which is likely due to differences in sediment grain size and water content that affected the occurrence of taxa. However, variable resolution of video imagery may skew some of these data, such as estimates of burrow density and minimum size. Our ability to discern burrows, especially small ones, was negatively affected at sites with poor image resolution because of high ship drift, turbidity in the water column, or both. Small burrows may well have been present but not detectable from the imagery. Similar limitations of benthic imagery have been pointed out elsewhere (e.g. Beisiegel et al., 2017). Thus, despite the development of visual recognition software and other tools that can provide guidance on optimal strategies for seafloor imagery acquisition (Perkins et al., 2016), ultimately, seafloor video is not a replacement for physical collections; the advantages seem to lie in scale of coverage.

The combined results from qualitative and quantitative analyses were clearly useful, for example in characterizing epibenthic habitats and identifying spatial patterns. Habitats dominated by brittle stars occur to the southwest of Saint Lawrence Island where a polynya persists in the winter, whereas mobile and sessile epifaunal communities

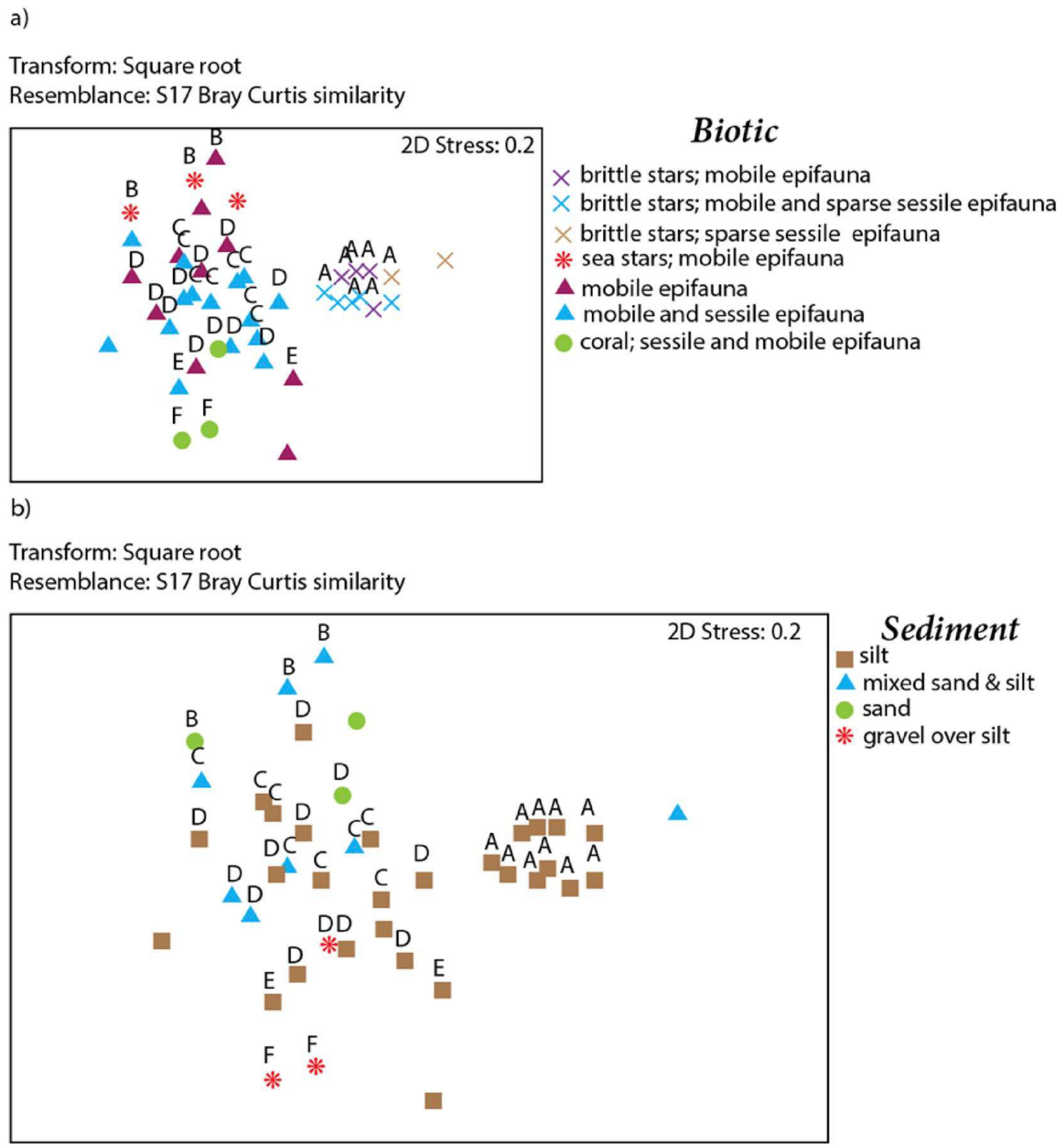

Fig. 6. a) MDS plot of video-produced epifaunal count data from 2008 with symbols representing biotic habitat descriptions and labeled by cluster. Cluster A represents stations dominated by brittle stars. b) MDS plot of epifaunal count data with symbols representing sediment descriptions and labeled by cluster showing that sediment types do not contain exclusively distinct epifaunal groups.

Table 2
Brittle star summary data from video quantitative analysis of HLY0802 sites. Biomass estimated using averaged mass per individual data collected in epibenthic trawls in the study area during a 2007 cruise of the USCGC *Healy* (Lovvorn et al., 2016, HLY0702). We used a conversion factor of 0.53 to convert number per m^2 to biomass. We used a species-specific conversion factor of 0.014 to convert biomass to carbon biomass (Stoker, 1978).

HLY 0802 Station Number	Station Name	N (still frames)	Taxa	Density (no/m^2)	Wet Wt. Biomass (g/m^2)	Carbon biomass (gC/m^2)	LAT (°N)	LON (°W)
35	STLAW	40	*Ophiura sarsi*	180.57	95.70	1.34	62.783	−174.348
36	SL14	40	*Ophiura sarsi*	0.67	0.35	0.00	62.2218	−175.937
36	SL14	40	*Ophiura* sp. (small)	300.65	159.34	2.23	62.2218	−175.937
38	SL12	22	*Ophiura sarsi*	30.55	16.19	0.23	62.1918	−175.129
38	SL12	22	*Ophiura* sp. (small)	18.14	9.61	0.13	62.1918	−175.129
39	SL11	40	*Ophiura sarsi*	58.77	31.15	0.44	62.1932	−174.634
39	SL11	40	*Ophiura* sp. (small)	245.06	129.88	1.82	62.1932	−174.634
40	SL10	40	*Ophiura sarsi*	24.30	12.88	0.18	62.1447	−173.996
58	W7	40	*Ophiura* sp. (small)	598.46	317.18	4.44	59.9997	−171.058
59	W8	39	*Ophiura* sp. (small)	558.98	296.26	4.15	59.8883	−171.296
110	ICE	40	*Ophiura sarsi*	41.13	21.80	0.31	62.2607	−172.558
111	70m58	40	*Ophiura sarsi*	70.52	37.37	0.52	62.1968	−174.709
111	70m58	40	*Ophiura* sp. (small)	20.43	10.83	0.15	62.1968	−174.709
116	70m53	40	*Ophiura sarsi*	97.87	51.87	0.73	61.5625	−173.715
116	70m53	40	*Ophiura* sp. (small)	50.60	26.82	0.38	61.5625	−173.715

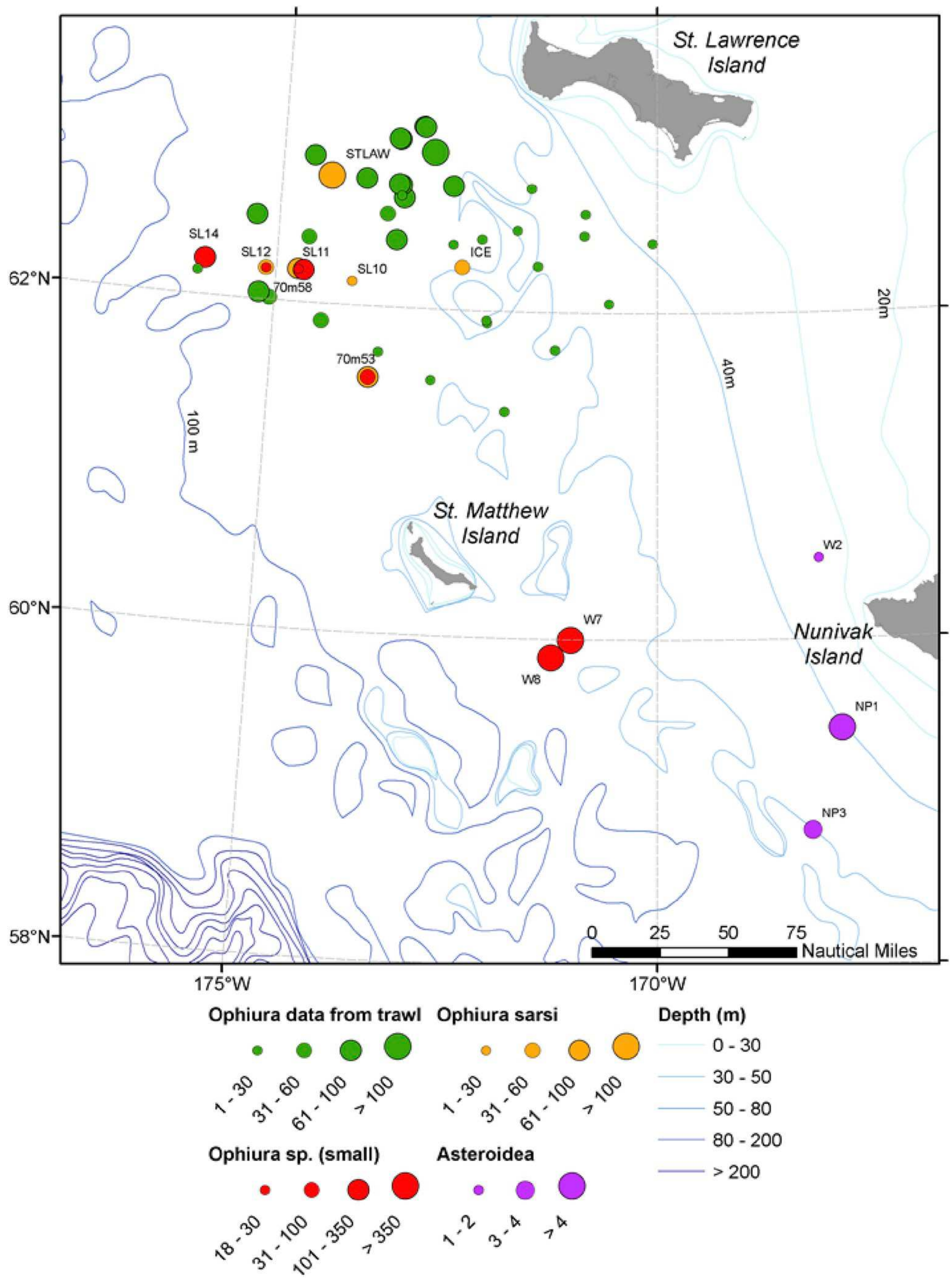

Fig. 7. Densities of brittle and sea stars (red, yellow and violet circles; all video data) in the study area labeled with the station numbers from HLY0801 and HLY0802 in 2008. Comparable trawl data (green circles) are from HLY0702 in 2007). Abundance data from video are presented in Table 2. (For interpretation of the references to colour in this figure legend, the reader is referred to the Web version of this article.)

Table 3
Sea star summary data from video quantitative analysis of HLY0802 sites.

Station Number	Station Name	N (still frames)	Taxa	Density (#/m^2)	Latitude°N	Longitude°W
15	NP1	40	Asteroidea	7.75	59.4552	192.2058
53	W2	40	Asteroidea	1.46	60.4992	192.0087
63	NP3	40	Asteroidea	3.76	58.8245	191.8027

(e.g. crabs, gastropods, tunicates) were found to the east. The polynya is thought to be associated with fine deposition and slow currents, whereas stronger currents and more coarse grain sediments are found to the east (Grebmeier and Cooper, 2016b); our video observations are consistent with these expectations. Comparisons with existing benthic infaunal data also indicate significant divisions among benthic communities in the western, eastern, and northern regions of the Saint Lawrence Island polynya (Grebmeier and Barry, 2007; Grebmeier and Cooper, 2016b). The western infaunal group is the most productive and is dominated by nuculanid, nuculid, and tellinid bivalves, and orbiniid polychaetes (Grebmeier and Barry, 2007; Grebmeier and Cooper, 2016b; Lovvorn et al., 2018). Northern and eastern groups also include nuculanid and nuculid bivalves, along with amphipods and cumaceans, but at a much lower mean biomass (Grebmeier and Barry, 2007). Similarities in spatial community separation suggest a potential link between infaunal and epifaunal communities through trophic interactions or the influence of environmental parameters on both communities at

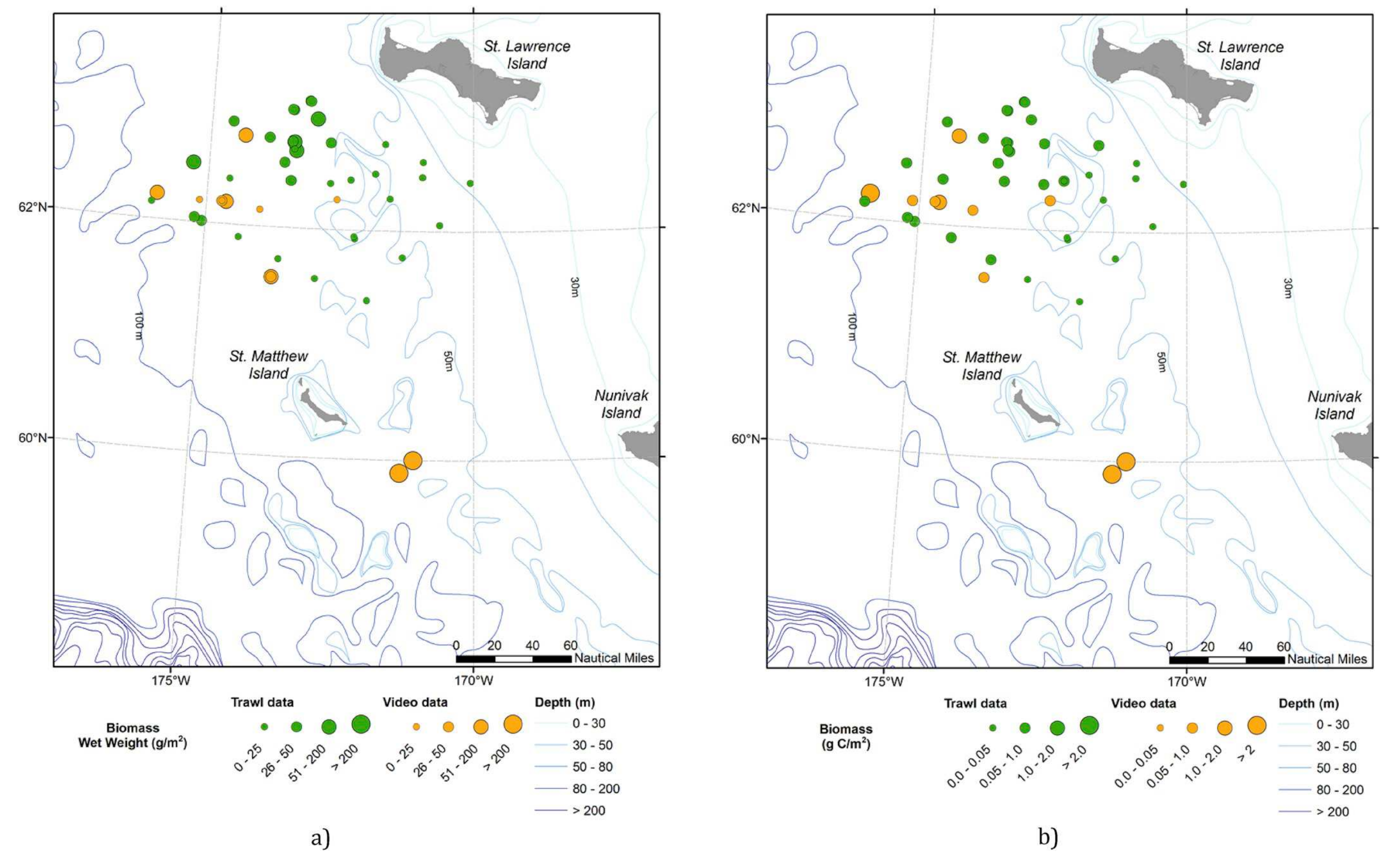

Fig. 8. Comparison of brittle star biomass: a) wet weight, g/m^2 and b) carbon ($g\ C/m^2$) collected from beam trawls during a 2007 cruise of the USCG *Healy* and this study in the Bering Sea. Video source data are presented in Table 2.

Table 4
Comparison of small-scale topography at brittle star, sea star, and other sites (Site type, bs = brittle stars, ss = sea stars, o = other—not dominated by brittle stars or sea stars) n = number of frames evaluated.

Station	Station Name	N	Site type	Burrow density	Burrow min diameter	Burrow max diameter	Pit density	Pit min diameter	Pit max diameter
35	STLAW	40	bs	207.82	0.18	0.39	25.39	2.48	2.62
36	SL14	40	bs	73.46	0.27	0.39			
38	SL12	22	bs	53.24	0.39	0.67	0.26	0.16	0.30
39	SL11	40	bs	972.40	0.19	0.39	13.58	1.06	1.50
58	W7	40	bs	512.26	0.18	0.35	36.26	1.67	2.59
59	W8	39	bs	1615.31	0.11	0.30	38.60	2.03	2.91
110	ICE	40	bs	699.35	0.14	0.48	31.14	1.06	0.12
111	70m58	40	bs	53.65	0.23	0.44	0.73	0.10	0.14
116	70m53	40	bs	367.76	0.22	0.36	0.38	3.75	3.75
15	NP1	40	ss	15.43	0.05	0.15			
53	W2	40	ss	396.49	0.18	0.25			
63	NP3	40	ss						
17	MN1	39	o	917.99	0.13	0.24			
28	MN12	40	o	184.30	0.33	1.09	1.83	0.40	0.57
46	SL6	40	o	564.49	0.17	0.57	6.99	0.42	0.60
47	SL5	40	o	1568.85	0.18	0.47	2.55	0.13	0.17
48	SL4	40	o	1795.05	0.19	0.36	0.40	0.15	0.23
49	NP7	12	o	41.90	0.77	0.85			

similar scales (Lovvorn et al., 2016). Patterns in hydrodynamics and/or sea ice and, therefore, carbon supply, are potential driving factors. For example, the observation that sediment grain size and the association of sediment organic carbon in surface sediments can be a good predictor of benthic community structure (Lovvorn et al., 2018) is related to the high biomass of brittle stars in soft organic muds southwest of St. Lawrence Island.

In addition, the video imagery identified locations with important epifaunal predators (i.e. sea stars) and areas that may represent transition zones between epifaunal communities and habitats, particularly in the more eastern locations occupied (Fig. 9). By contrast, in soft muds to the southwest of Saint Lawrence Island, brittle stars were dominant. Southwest of Saint Matthew Island is the only area where we observed mixed gravel and coral communities (Fig. 9). Stations near Nunivak Island generally contained more coarse-grained sediments than those to the south of St. Lawrence Island and include sites dominated by sea stars (Fig. 9). The most southerly regions have mixed sediment types and epifaunal communities. Some of these differences are probably due to the influence of different water masses, specifically Alaska Coastal Water and Bering Shelf Water, which are fresher and

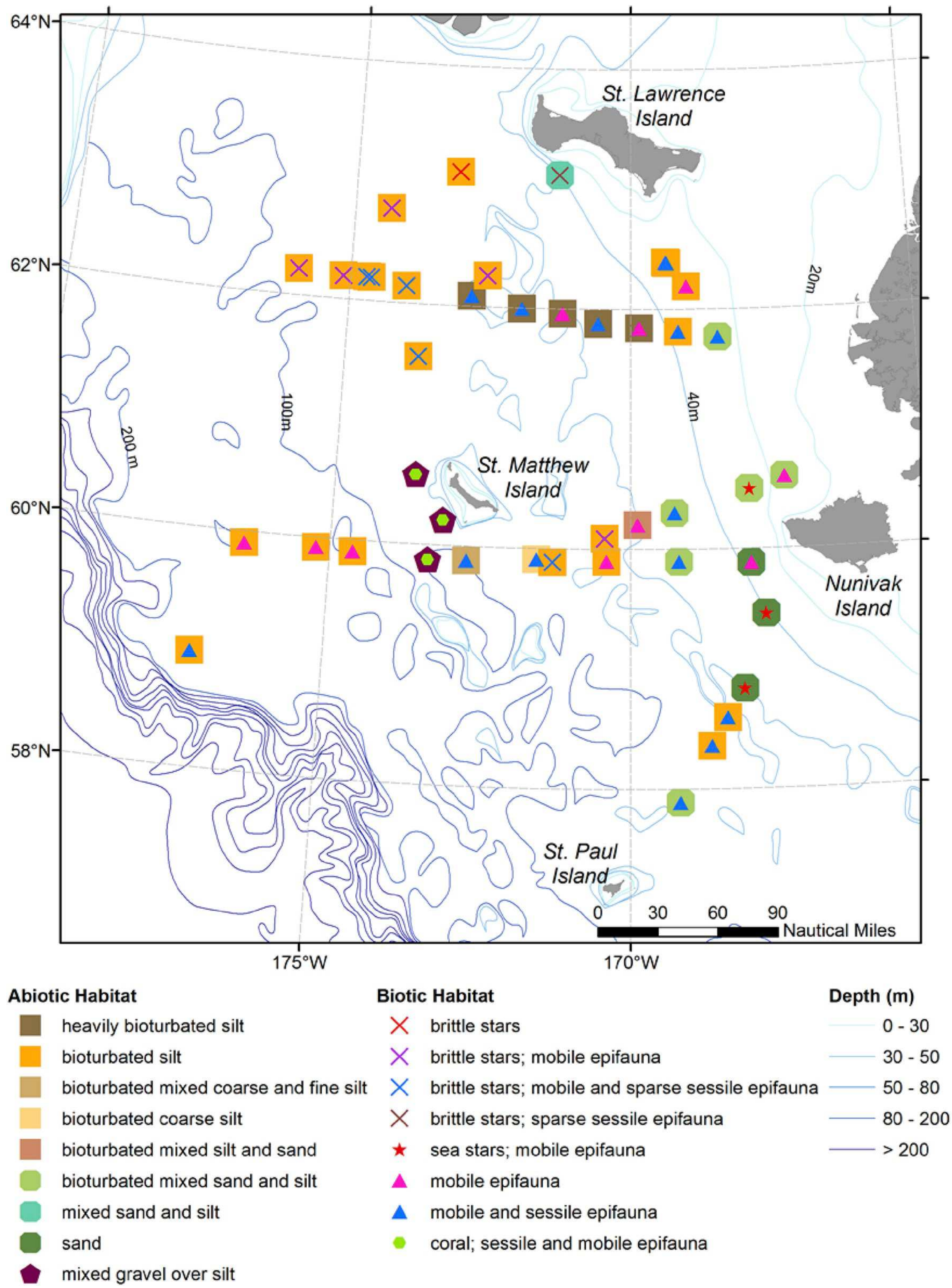

Fig. 9. Abiotic and biotic habitat descriptions from qualitative analysis of video images. A one-to-one relationship is evident between coral and mixed gravel over silt habitats. Heavily bioturbated sediments were only found to the southeast of St. Lawrence Island in mobile and sessile epifauna habitat. The most southerly regions have mixed sediment types and epifaunal communities.

decline in nutrients closer to the Alaska coast. These water mass differences can influence underlying benthic communities, which show the highest productivity in benthic "hot-spots" (reviewed by Grebmeier et al., 2015). The identification of these habitats in more detail than provided by simple cluster analysis (e.g. "mobile and sessile epifauna") highlights the potential for additional habitat characterizations. For example, a one-to-one relationship is evident between coral and mixed gravel over silt habitats. Heavily bioturbated sediments were only found in the eastern area of the SLIP in mobile and sessile epifauna habitat.

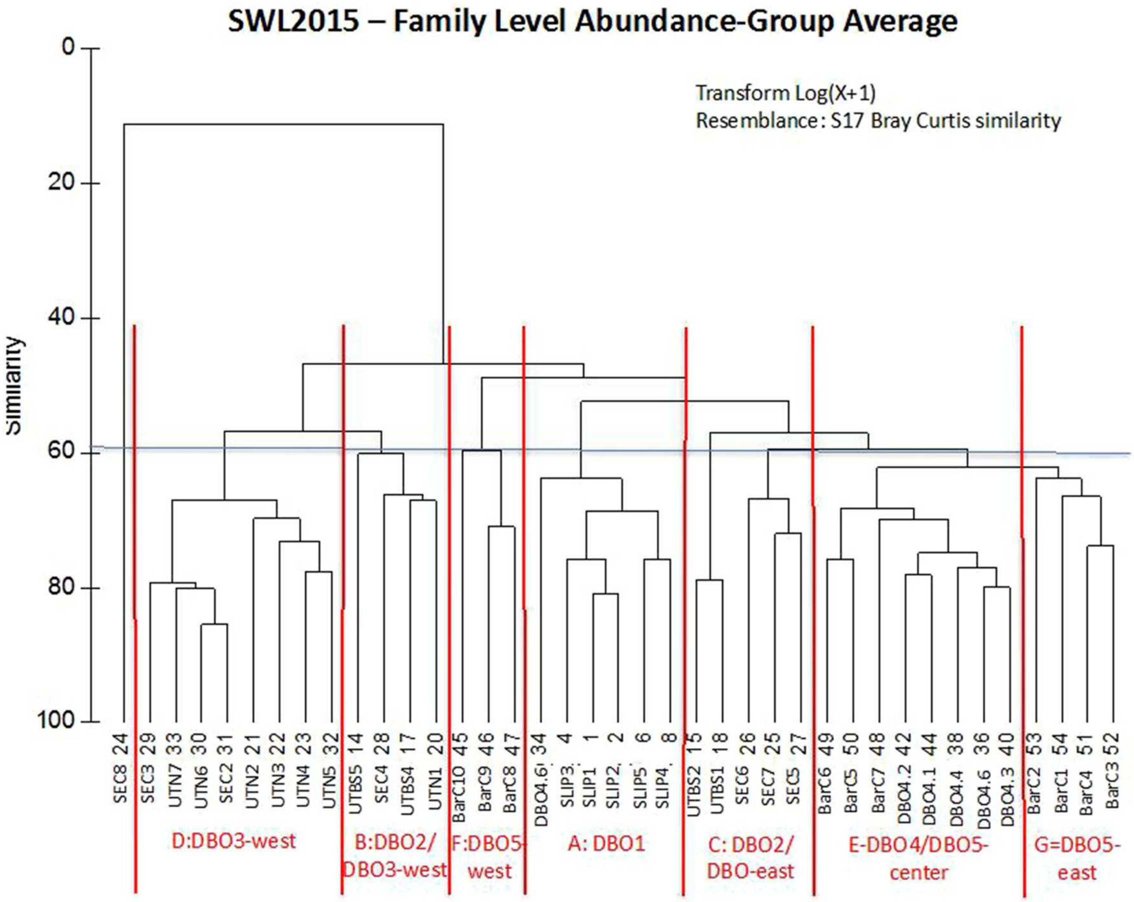

Fig. 10. Cluster analysis of macrobenthic communities from the *Sir Wilfrid Laurier* 2014 cruise indicating 7 major groupings used as a qualitative descriptor for the video efforts from the *Sir Wilfrid Laurier* (SWL) in 2016 and 2017 (see Table 5 and methods section).

3.2. Distributed Biological Observatory sampling, 2016–2017

Benthic identification and biomass measurements completed in the lab from sampling in 2014 indicate that the benthic communities studied clustered into seven groups using PRIMER (Figs. 10, 11), so there was overlap among the 5 DBO regions (DBO1 to DBO5; Fig. 2), which were occupied for video imagery generation in 2016 and 2017 as described previously. Those video observations, including similarities and differences among time series stations within each DBO region, are detailed in Table 5, and described in aggregate in the following section. Comparing among the five DBO regions, DBO 1 (south of St. Lawrence Island) is muddy, and dominated by brittle stars; DBO 2 is coarser grained due to higher currents and has high nutrient concentrations increasing to the west; DBO3 includes stations where settling material that has transited through Bering Strait is deposited; DBO4 has heterogeneous sediments and epifauna, with finer, muddy sediments offshore, and filter feeders favored in the coarser sediments inshore; and DBO5 has the undersea Barrow Canyon feature through which Bering Sea waters flow into the offshore Arctic Ocean, and it is also a source of Atlantic layer upwelling. Each of these DBO regions are considered to be "hotspots" of productivity with regular observations being undertaken to evaluate biological community changes (Grebmeier et al., 2010).

DBO1: These five time series stations, which are influenced by the St. Lawrence Island winter polynya (SLIP) were all clustered in Group A (Fig. 10). All bottom water temperatures were < -0.5 °C, sediments were underlain by silt and clay, and station depths ranged from 70 to 80 m. Epibenthic fauna, in composite, were characterized by numerous brittle stars, less numerous sea stars, as well as polychaetes, hermit crabs, opilio crabs, and moon snails.

DBO2: These time series stations north of St. Lawrence Island, but south of Bering Strait (Chirikov Basin) were clustered into two groups: a western one (B; stations UTBS5, UTBS4) and an eastern one (C: stations UTBS1, UTBS2, UTBS2A, and DBO2.7). The western cluster group B was characterized by bottom water temperatures during filming from 1.2 to 3.3 °C, silty-sand sediments, and station depths ranging from 46 to 48 m. Epibenthic fauna included sea stars, ampharetid worm tubes, sea stars, numerous small crabs, a few sculpin fish, tube anemones, tunicates, gastropods, as well as phytoplankton floc on surface sediments. In 2017, there was also an euphausiid (krill) and/or copepod swarm near the bottom, as well as many ctenophore carcasses. By comparison, the eastern cluster group C was characterized by bottom water temperatures during filming from 0.6 to 3.5 °C, sandy-silt sediments, and station depths ranging from 38 to 48 m. Epibenthic fauna included numerous small crabs, a few sea anemones, tunicates, the "string" bryozoan *Alcyonidium vermiculare*, gastropods, and hermit crabs. There was also noticeable phytoplankton floc present on and above the sediments.

DBO3: Located in the SE Chukchi Sea, this region had a transitional cluster (B) between a strongly defined western cluster (D) in the offshore region and a cluster near the Alaska coastline (C). Specifically, the transitional stations (UTN2 and SEC4) had bottom water temperatures during filming from 3.3 to 3.5 °C, sandy silt and clay sediments, and a bottom depth from 34 to 52 m. Epibenthic fauna included sand dollars, *Opilio* crabs, snails, and basket stars. The remaining groups (E and F) in DBO3 were separated as follows: the western group E stations (UTN2-7, SEC2, SEC3) and the eastern group F stations (SEC5-7). The western cluster group E was characterized by bottom water temperatures during

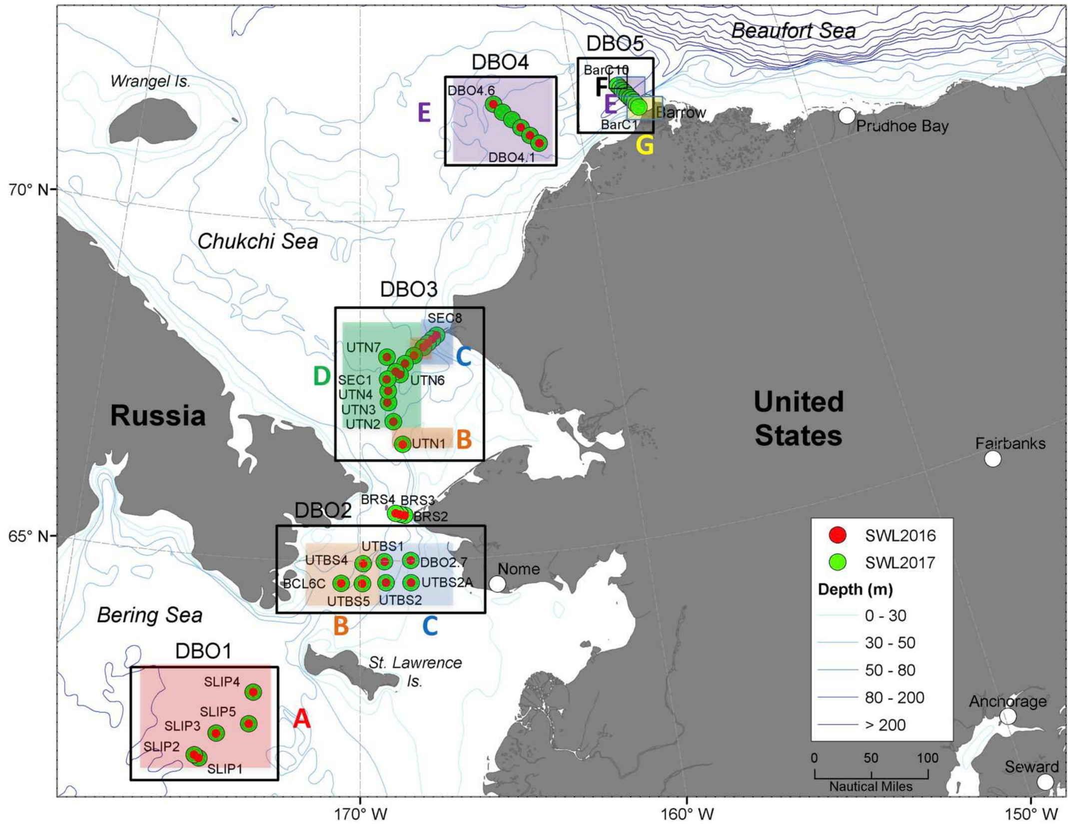

Fig. 11. Schematic of the qualitative cluster groupings based on macrofaunal data for the Sir Wilfrid Laurier (SWL) 2014 cruise using PRIMER statistical software (see methods and Fig. 10). These data were used to separate qualitatively the epifaunal communities that were filmed. Boxes with labels A, B, C, D, E, F, G correspond to clusters identified; station within each box were sampled in 2016 (smaller red circles) and 2017 (larger green circles) from the *Sir Wilfrid Laurier* (SWL). (For interpretation of the references to colour in this figure legend, the reader is referred to the Web version of this article.)

filming from 1.6 to 2.5 °C, silt and clay/sandy sediments, and station depths ranging from 38 to 48 m. Epibenthic fauna included bivalves, *Serripes* sp. (evidenced by siphon holes), numerous empty *Macoma* clam shells, brittle stars, small fish, sea stars, crabs, sea anemones, a few hermit crabs, and prominent marine snow in the benthic nepheloid layer. The eastern group (F) was characterized by bottom water temperatures during filming from 5.3 to 6.6 °C, coarse sand and gravel sediments, and depths ranging from 43 to 49 m. Epibenthic fauna, included tube anemones, crabs, *Psolus* sea cucumbers, basket stars, sea peach tunicates, tube anemones, a few sea urchins and small fish, including flatfish.

DBO4: This region was located in the NE Chukchi Sea. Group G included all DBO4 stations and was characterized by bottom water temperatures during filming that ranged from −0.9 to 3.8 °C, variable sediment type from silt and clay to coarse sand and gravel, and depths ranging from 41 to 46 m. Epibenthic fauna were dominated by brittle stars, some sea stars, tube anemones, the sea cucumber, *Psolus* sea cucumbers, basket stars, soft coral (sea raspberry), gastropod snails (*Neptunea)*, and in many locations, a prominent phytoplankton floc was visible on sediments.

DBO5: Located in Barrow Canyon, this area was only occupied completely in 2017 as there was heavy ice over it in July 2016 that inhibited sampling. We did not evaluate cluster groupings, but there is high biodiversity across the canyon from west to east, based upon a distinct west to east contrast in many variables. The western side of Barrow Canyon (BarC6-10) had bottom water temperatures during filming of −0.6 to 0.1 °C, silt and clay sediments, with depths ranging from 62 to 111 m. Epibenthic fauna included brittle stars, tube anemones, soft corals (sea raspberry), sea anemones, some clam shells, serpulid worms, and in bottom waters, a prominent plankton floc, including decaying ctenophore carcasses. The central station (BarC5) over the canyon axis had a bottom water temperature at the time of filming of 1.9 °C, silt and clay sediment over coarse-grained gravel, and a depth of 120 m. Epifauna included a high biodiversity of brittle stars, soft corals (sea raspberry), bryozoans including *Alcyonidium vermiculare*, and other species, hermit crabs, and snail egg masses. The eastern BC stations (BarC1-4) had warmer bottom water temperatures (4.3–6.1 °C), mixed silt and clay and much coarser sediments, from sand to gravel, with a depth range from 46 to 111 m. Epifauna included brittle stars, *Psolus* sea cucumbers, soft corals (sea raspberry), sea urchins, basket stars, *Opilio* crabs, fish, small pink sea cucumbers, sea anemones, king crabs, hermit crabs, solitary corals, *Boltenia* tunicates, hermit crab, and bryozoans. Chaetognaths and euphausiids were also visible in the bottom water column.

Short edited segments from each DBO station are available at: https://www.youtube.com/watch?v=wT2BwdE6K00 (2016) and https://www.youtube.com/watch?v=QGvJm1VjGrk&t=243s (2017). In addition, the full digital files for each DBO station are accessible at: https://drive.google.com/drive/folders/16Q9oAM1e-fgQQmK6JG7xPxtdm9MjdEn1 (2016) and https://drive.google.com/drive/folders/1nk1TNsyY1acKPfGdVkJp4K0Ifov7cgE_ (2017).

4. Conclusions

A key goal of this project was to test the utility of this underwater camera system for characterizing epifaunal assemblages on a vast soft-bottom continental shelf. Our deployment approach (i.e. one hand-deployed drop per station while the ship was drifting for approximately 10 min) provided useful habitat characterizations (sediments and faunal composition) at the scale of the sampling station (0.5 nautical miles). Many projects with similar goals utilize video data in combination with acoustic data to create larger scale habitat maps. These

Table 5
Qualitative cluster analysis based on environmental and faunal data descriptions in relation to clustering of macrofauna at same stations using SWL14 benthic data in Primer statistical software (see methods and Fig. 10).

Station	2016 Video Observations	2017 Video Observations
SLIP1 (A)	Temperature: -0.7 °C, Depth: 78 m Description: silt and clay sediments, numerous brittle stars (*Ophiura sarsi*, *Ophiura* sp.), crabs (*Chionoecetes sp*., hermit crabs), crabs	Temperature: -0.8 °C, Depth: 78 m Description: silt and clay sediments, euphausiids (krill), crustaceans, high marine snow, brittle stars (*Ophiura sarsii)*, phytoplankton floc (low), crab *Chionoecetes* sp.), sea anemone
SLIP2 (A)	Temperature: -0.8 °C, Depth: 80 m Description: silt and clay sediments, numerous brittle stars, sea star (*Asterias sp.),* polychaetes	Temperature: -0.8 °C, Depth: 80 m Description: silt and clay sediments, brittle stars (*Ophiura* spp.), small crabs, worm burrows, marine snow, moon snail egg casings
SLIP3 (A)	Temperature: -0.7 °C, Depth: 70 m Description: silt and clay sediments, numerous brittle stars (*Ophiura* spp.), sea stars, hermit crabs, crab, moon snails	Temperature: -0.9 °C, Depth: 71 m Description: silt and clay sediments, brittle stars (*Ophiura* spp.), marine snow, clam siphon holes, nemertean worms
SLIP5 (A)	Temperature: -0.7 °C, Depth: 65 m Description: silt and clay sediments, numerous brittle stars (*Ophiura* spp.), crabs, fish, bivalve siphon holes, moon snails, low marine snow	Temperature: -0.6 °C, Depth: 65 m Description: silt and clay sediments, hermit crabs (*Pagurus* sp.), brittle stars *Ophiura* spp.), Nemertean worms, clam siphons, sea anemones, worm traces
SLIP4 (A)	Temperature: -0.8 °C, Depth: 70 m Description: silt and clay sediments, numerous brittle stars (*Ophiura* spp.), crabs (*Chionoecetes* sp., *Hyas* sp.), nemertean worm	Temperature: -0.5 °C, Depth: 71 m Description: silt and clay sediments, brittle stars (*Ophiura* sp.), less marine snow, Nemertean worms, phytoplankton floc on sediments, moon snail casings, small fish
UTBS5 (B)	Temperature: 1.2 °C, Depth: 46 m Description: silt and clay/sandy sediments, sea stars, ampharetid worm tubes (F. Ampharetidae), abundant crabs, sculpin, other fish, tube anemones (*Ceriantharia* sp.), tunicates (F. Pyuridae), phytoplankton floc	Temperature: 2.7 °C, Depth: 47 m Description: silty sand sediments, large sculpin fish, phytoplankton floc on sediment surface, marine snow, ampharetid worm tubes
UTBS2 (C)	Temperature: 0.6 °C, Depth: 45 m Description: sandy sediments, abundant small crabs (*Chionoecetes sp* .), sea stars, bryozoans, hermit crabs, sea anemones, serpulid worms, phytoplankton floc	Temperature: 2.9 °C, Depth: 45 m Description: sandy sediments, hermit crabs, crabs, bryozoans, phytoplankton floc on sediment surface, sea stars, sea anemones, bryozoans, *Ampelisca* sp. amphipods tubes, tunicate (*Boltenia sp.*), clam shells
UTBS2A (C)	Temperature: 2.3 °C, Depth: 38 m Description: sandy silt sediments, numerous small crabs, sea anemone, bryozoans, gastropods, phytoplankton floc	Temperature: 2.3 °C, Depth: 38 m Description: sandy silt sediments, numerous small crabs (~3cm), sea cucumber (*Psolus*), sea anemone, bryozoans, hermit crabs, a few burrows
DBO2.7 (C) (near King Island)	Temperature: 2.8 °C, Depth: 44 m Description: sandy sediments, sea star, crabs, brittle stars (*Ophiura sarsi)*, basket stars (*Gorgonocephalus* sp.), bryozoans (*Alcyonidium vermiculare)*, sea anemones, surface phytoplankton floc	Temperature: 2.1 °C, Depth: 45 m Description: sandy sediments, string bryozoan (*Alcyonidium vermiculare)*, crabs, sea star, sea anemone, clam shell, hermit crab
UTBS4 (B)	Temperature: 1.7 °C, Depth: 48 m Description: silty sand sediments, crabs (*Chionoecetes* sp., *Hyas* sp.), sea anemones, surface phytoplankton floc, snails, serpulid worms, sea stars	Temperature: 3.3 °C, Depth: 48 m Description: silty sand sediments, phytoplankton floc, euphausids (krill) or copepod swarm, siphon holes, hermit crabs, sea anemones, ctenophore carcasses, marine snow, sea stars, sipunculid worms
UTBS1 (C)	Temperature: 0.6 °C, Depth: 48 m Description: sandy silt sediments, hermit crabs, phytoplankton floc on sediments, sea anemone, crab, sea star, string bryozoa, gastropods	Temperature: 3.5 °C, Depth: 48 m Description: sandy silt sediments, phytoplankton flock on sediments, sea anemone, serpulid worm, string bryozoan (*Alcyonidium vermiculare)*, hermit crab, holes for ampeliscid amphipods (*Ampelisca* sp.)
UTN1 (D)	Temperature: 3.5 °C, Depth: 34 m Description: silty sand sediments, lots of sand dollars (*Echinarachnius parma)*, sea anemone, sea star, snail, crab (*Chionoecetes sp*.)	Temperature: 4.6 °C, Depth: 34 m Description: silty sand sediments, sand dollars, crab (*Chionoecetes* sp.), snail, basket star (*Gorgonocephalus* sp.)
UTN2 (E)	Temperature: 2.5 °C, Depth: 45 m Description: sandy silt sediments, bivalve siphon holes, brittle stars (*Ophiura sarsi)*, fish	Temperature: (no temp or depth on video clip) Description: fast currents, sandy silt sediments, lots of *Macoma calcarea* shells, *Serripes sp.* siphon holes, brittle star (*Ophiura sarsii)*, small fish, sea star, crab (*Chionoecetes* sp.)
UTN3 (E)	Temperature: 1.6 °C, Depth: 49 m Description: sandy silt sediments, lots empty *Macoma calcarea* clam shells on surface, fast currents, lots turbidity	Temperature: 4.7 °C, Depth: 49 m Description: silt and clay sediments, *Macoma calcarea* clam shells, clam siphons, marine snow, polychaete burrows
UTN4 (E)	Temperature: 1.8 °C, Depth: 50 m Description : Silt and clay sediments, empty *Macoma calcarea* clam shells on surface, fast currents and swell	Temperature: 4.3 °C, Depth: 49 m Description: soft sediments, marine snow, ctenophore carcasses, lots empty bivalve shells (*Macoma calcarea)*, bivalve siphons, fish, murky water due to swells
SEC8 (single)	Temperature: 5.8 °C, Depth: 34 m Description: gravel and sandy sediments, sea star, basket stars, tube anemones (anemone, crab, fast currents	Temperature: 7.1 °C, Depth: 35 m Description: gravel and sand sediments, hermit crab (*Pagurus* sp.), sea star, basket star, tube and singular sea anemones, soft and hard corals, crab, sea urchin, serpulid worm, basket star
SEC7 (F)	Temperature: 6.6 °C, Depth: 43 m Description: gravel and sandy sediment, tube anemones, crabs, sea cucumber (*Psolus* sp.), tunicates, basket star, sea peach tunicate (F. Pyuridae), tube anemones, sea urchin,	Temperature: 6.0 °C, Depth: 43 m Description: gravely sand sediments, phytoplankton flock on sediment, sea peach tunicate, scallop shells, tube anemone, basket star
SEC6 (F)	Temperature: 6.4 °C, Depth: 47 m Description: coarse sediments/gravel, basket star, sea raspberry, crab, sea cucumber (*Psolus* sp.), tunicate, tube anemone (*Ceriantharia* sp.), sea peach tunicate (F. Pyuridae), sea urchin (*Strongylocentrotus* sp.)	Temperature: 5.3 °C, Depth: 47 m Description: gravely sand sediments, basket stars, scallop, clam, sea urchin, tunicates, crab, hermit crab, brittle star (*Ophiura sp*.), sea cucumber, gastropod
SEC5 (F)	Temperature: 5.3 °C, Depth: 49 m Description: coarse sediments/gravel/rocks, sea peach tunicate, tube anemones (*Ceriantharia* sp.), gastropod, sea anemones, sea urchin, small fish, flatfish	Temperature: 4.6 °C, Depth: 50 m Description: gravely sand sediments, large crab, sea urchin, open clam shell, tunicates, basket stars

(*continued on next page*)

Table 5 (*continued*)

Station	2016 Video Observations	2017 Video Observations
SEC4 (E)	Temperature: 3.3 ˚C, Depth: 52 m Description: silt and clay/sand, phytoplankton flock, clam shells on surface, sea star, crab, fish,	Temperature: 4.1 ˚C, Depth: 53m Description: gravely sand sediments, hermit crab, snail egg casings, fast currents, small fish, sand dollars, phytoplankton flock, string *Bryozoa*, basket star
SEC3 (E)	Temperature: 1.5 ˚C, Depth: 57 m Description: silt and clay/sand sediments, fast currents and high turbidity, so poor video, see empty clam shells on surface	Temperature: 4.5 ˚C, Depth: 58 m Description: silt and clay sediments, brittle stars, sea anemone, lots of clam siphon holes
UTN6 (E)	Temperature: 3.3 ˚C, Depth: 52 m Description: silt and clay sediments, sea star, sea anemone, snail, clam siphon holes, surface flock, sea star, fish,	Temperature: 4.1 ˚C, Depth: 46 m Description: silt and clay, sea star, sea anemone, lots of clam siphon holes
SEC2 (E)	Temperature: 1.6 ˚C, Depth: 50 m Description: silt and clay sediments, sea stars, ctenophore carcasses, snail, clam siphon holes, sea anemones	Temperature: 4.0 ˚C, Depth: 50 m Description: high silt and clay, hermit crab, siphon holes, lots of sea anemones, fish, crabs, worm or amphipod tubes, murky waters
UTN5 (SEC1-"hotspot") (E)	Temperature: 1.8˚C, Depth: 50 m Description: sediments-, fish, sea anemones, empty white clam shells (*Macoma* spp.), hermit crab, sea stars, fish	Temperature: 4.1 ˚C, Depth: 50 m Description: silt and clay sediments, fast currents thus high turbidity, sea star, marine snow, fish, sea anemone, clam shells on surface, siphon holes
UTN7 (E)	Temperature: 1.1 ˚C, Depth: 57 m Description: silt and clay sediments, fish, high suspended low, so poor video	Temperature: 4.4 ˚C, Depth: 57 m Description: silt and clay sediments, hermit crab, sea stars, crabs, sea anemones
DBO4.6 (G)	Temperature: -0.8 ˚C, 41 m Description: sand, silt and clay, gravel sediments, lots brittle stars, crabs, gelatinous balls	Temperature: 1.8 ˚C, Depth: 41 m Description: silty sand sediments/gravel , gastropod snail (*Neptune asp.)*, sea stars, tube anemone (*Ceriantharia* sp.), phytoplankton flock, basket star, brittle stars (*Ophiura* spp.)
DBO4.5 (G)	No data due to ice cover	Temperature: 1.9 ˚C, Depth: 42 m Description: sand and silt/clay sediments, lots of brittle stars, tube anemones, sea cucumber (*Psolus sp.*), sea raspberry soft coral
DBO4.4 (G)	No data due to ice cover	Temperature: 1.7 ˚C, Depth: 45 m Description: sand and silt/clay sediments, abundant brittle stars, hermit crabs, sea stars, crabs, *Psolus* sea cucumber
DBO4.3 (G)	Temperature: -0.9˚ C, Depth: 45 m Description: sand and silt/clay sediments, numerous brittle stars, basket stars, soft corals (sea raspberry), sea stars	Temperature: 2.0 ˚C, Depth: 45 m Description: silty sand sediments, *Psolus* sea cucumbers, abundant brittle stars, sea stars, tube anemones
DBO4.2 (G)	Temperature: -0.8˚ C, Depth: 45 m Description: sand and silt/clay sediments, abundant brittle stars, crab, sea anemones, tube sea anemones,	Temperature: 3.0 ˚C, Depth: 46 m Description: sand and silt/clay sediments, brittle stars, sea anemones
DBO4.1 (G)	Temperature: -0.7˚ C, Depth: 44 m Description: sand and silt/clay sediments, numerous brittle stars, basket stars, sea cucumber (*Psolus sp.)*	Temperature: 3.8˚C, Depth: 45 m Description: sand and silt/clay sediments sea stars, abundant brittle stars, tube sea anemones, *Psolus* sea cucumber, phytoplankton floc on sediments
BarC10	No sampling, too much sea ice cover	Temperature: -0.6 ˚C, Depth: 62 m Description: silty clay sediments, ctenophore carcasses, brittle stars, tube anemones against strong current
BarC9	No sampling, too much sea ice cover	Temperature: -0.3˚C, Depth: 64 m Description: silt and clay sediments, a lot of marine snow, ctenophore carcasses, brittle stars, tube anemones
BarC8	No sampling, too much sea ice cover	Temperature: 0.1˚C, Depth: 71 m Description: silt and clay sediments, numerous brittle stars, marine snow, phytoplankton floc, ctenophore carcasses
BarC7	No sampling, too much sea ice cover	Temperature: -0.4˚C, Depth: 83 m Description: silt and clay sediments, numerous brittle stars, sea raspberry (*Gersemia rubiformis*), marine snow, clump of sponges, ctenophore carcasses, tube anemones, serpulid worm
BarC6	No sampling, too much sea ice cover	Temperature: -0.5˚C, Depth: 111 m Description: lots of brittle stars, marine snow, phytoplankton flock, sea raspberry, sea anemones, some clam shells
BarC5	No sampling, too much sea ice cover	Temperature: 1.9˚C, Depth: 120 m Description: silt and clay sediment over coarser sediments, numerous brittle stars (*Ophiura* sp.), abundant sea raspberry specimens (*Gersemia rubiformis)*, bryozoans,
BarC4	No sampling, too much sea ice cover	Temperature 4.3˚C, Depth: 111 m Description: silt and clay sediments over coarser sediment/gravel/rocks, brittle stars, *Psolus* (sea cucumber), soft coral (expanded sea raspberry), sea urchins, basket stars, crabs, fish, chaetognaths in water, euphausids
BarC3	No sampling, too much sea ice cover	Temperature: 4.9˚C, Depth: 91 m Description: coarse sand and gravels, rocks, lots of small, pink sea cucumbers (*Ocnus glacialis)*, sea cucumber (*Psolus* sp.), crabs, sea anemones, king crabs
BarC2	No sampling, too much sea ice cover	Temperature: 6.1˚C, Depth: 57 m Description: gravely sediment with pebbles and rocks, sea cucumber (*Psolus* sp.), sea raspberry (*Gersemia rubiformis)*, krill, hermit crab, solitary coral, sea urchin, fish
BarC1	No sampling, too much sea ice cover	Temperature: 6.1˚C, Depth: 46 m Description: coarse sediment and rocks, fast current, tunicates (*Boltenia* sp.*)*, sea raspberry (*Gersemia rubiformis)*, sea anemone, hermit crab, crab, bryozoans

studies often use specific video transect lines (e.g. Hewitt et al., 2004; Kendall et al., 2005) and positional tracking devices such as digital GPS (dGPS) and ultra-short baseline (USBL) transponders (for examples using dGPS see Hewitt et al., 2004; Brown and Collier, 2008; Strong and Lawton, 2004); for USBL example see McGoningle et al. (2009). These approaches facilitate geo-referencing of video data, development of image mosaics, and more sophisticated quantitative analyses than was possible within the scope of this project.

In this study, we met our initial objective of demonstrating the use of benthic video data to characterize epibenthic assemblages in the Bering Sea. These imagery files are useful for identification of broad- and local-scale benthic spatial patterns and improve upon infaunal data alone. These patterns show large-scale biological community transformations over DBO transect lines, including shifts from deposit feeding organisms such as brittle stars in soft muddy sediments to filter feeding organisms such as tunicates and sea anemones in waters near the Alaska coastline. This was particularly evident in two of the DBO transects, DBO4 and BarC, which are transect lines that cross water mass boundaries in the Chukchi Sea. Specifically, in nearshore areas there is less particle deposition under the fast-moving Alaska Coastal Current, so filter feeding organisms have an advantage over deposit feeders. These imaging data may also be useful over time for tracking shifts in both epifaunal and infaunal communities, following this documentation of reference conditions. Mobile epifauna are not as strongly coupled to the overlying water column as infauna and it is reasonable to assume that changes in seasonal sea ice duration might result in mobile epifauna migrating north of their historical distributions (Grebmeier et al., 2006). Such changes in ice conditions could be accompanied by a decreased food supply to the benthos with effects on both mobile epifaunal and infaunal communities.

Acknowledgments

We thank the North Pacific Research Board for funding the purchase of the camera system, and the US National Science Foundation (OPP 1204082, OPP1702456), and NOAA for research support that facilitated the video filming. The Canadian Coast Guard personnel aboard the CCGS *Sir Wilfrid Laurier* were instrumental in deploying the camera system and ship handling that significantly improved the video quality achieved. We thank Ed Davis (NOAA) and Dr. Boris Sirenko (Zoological Institute, Russian Academy of Sciences, St. Petersburg) for their shipboard efforts in deploying the epibenthic camera system and van Veen grabs for infaunal collections made during both Healy cruises in 2008. Christian Johnson is also thanked for the assistance he provided with some of the videography. Finally, we thank two anonymous reviewers who provided comments that helped to improve the manuscript.

References

Beisiegel, K., Darr, A., Gogina, M., Zettler, M.L., 2017. Benefits and shortcomings of non-destructive benthic imagery for monitoring hard-bottom habitats. Mar. Pollut. Bull. 121, 5–15.

Bluhm, B.A., Iken, K., Mincks Hardy, S., Sirenko, B.I., Holladay, B.A., 2009. Community structure of epibenthic megafauna in the Chukchi Sea. Aquat. Biol. 7, 269–293.

Brown, C., Collier, J., 2008. Mapping benthic habitat in regions of gradational substrata: an automated approach utilizing geophysical, geological, and biological relationships. Estuar. Coast Shelf Sci. 78, 203–214.

Cui, X., Grebmeier, J., Cooper, L., Lovvorn, J., North, C., Seaver, W., Kolts, J., 2009. Spatial distributions of groundfish in the northern Bering Sea in relation to environmental variation. Mar. Ecol.: Prog. Ser. 393, 147–160.

Durden, J.M., Bett, B.J., Schoening, T., Morris, K.J., Nattkemper, T.W., Ruhl, H.A., 2016. Comparison of image annotation data generated by multiple investigators for benthic ecology. Mar. Ecol.: Prog. Ser. 552, 61–70.

Feder, H.M., Jewett, S.C., Blanchard, A., 2005. Southeastern Chukchi sea (Alaska) epibenthos. Polar Biol. 28, 402–421.

Glover, A.G., Gooday, A.J., Bailey, D.M., Billett, D.S.M., Chevaldonné, P., Colaço, A., Copley, J., Cuvelier, D., Desbruyères, D., Kalogeropoulou, V., Klages, M., Lampadariou, N., Lejeusne, C., Mestre, N.C., Paterson, G.L.J., Perez, T., Ruhl, H., Sarrazin, J., Soltwedel, T., Soto, E.H., Thatje, S., Tselepides, A., Van Gaever, S., Vanreusel, A., 2010. In: Lesser, M. (Ed.), Chapter One - Temporal Change in Deep-Sea Benthic Ecosystems: A Review of the Evidence from Recent Time-Series Studies. Adv. Mar. Biol.. Academic Press, pp. 1–95.

Gomes-Pereira, J.N., Auger, V., Beisiegel, K., Benjamin, R., Bergmann, M., Bowden, D., Buhl-Mortensen, P., De Leo, F.C., Dionísio, G., Durden, J.M., Edwards, L., Friedman, A., Greinert, J., Jacobsen-Stout, N., Lerner, S., Leslie, M., Nattkemper, T.W., Sameoto, J.A., Schoening, T., Schouten, R., Seager, J., Singh, H., Soubigou, O., Tojeira, I., van den Beld, I., Dias, F., Tempera, F., Santos, R.S., 2016. Current and future trends in marine image annotation software. Prog. Oceanogr. 149, 106–120.

Grebmeier, J.M., 2012. Shifting patterns of life in the Pacific Arctic and sub-arctic seas. Ann. Rev. Mar. Sci. 4, 63–78.

Grebmeier, J.M., Barry, J.P., 2007. Benthic processes in polynyas. In: Smith, W.O., Jr, Barber, D.G. (Eds.), Polynyas: Windows to the World. Elsevier, Amsterdam, pp. 363–390.

Grebmeier, J.M., Bluhm, B.A., Cooper, L.W., Denisenko, S.G., Iken, K., Kędra, M., Serratos, C., 2015. Time-series benthic community composition and biomass and associated environmental characteristics in the Chukchi sea during the RUSALCA 2004–2012 program. Oceanogr 28, 116–133.

Grebmeier, J., Cooper, L., 2016a. PacMARS Surface Sediment Parameters. Version 2.0. UCAR/NCAR - Earth Observing Laboratory. https://doi.org/10.5065/D6416V3G.

Grebmeier, J.M., Cooper, L.W., 2016b. The Saint Lawrence Island polynya: a 25-year evaluation of an analogue for climate change in polar regions. In: Glibert, P.M., Kana, T.M. (Eds.), Aquatic Microbial Ecology and Biogeochemistry: A Dual Perspective. Springer International Publishing, Cham, pp. 171–183.

Grebmeier, J.M., Cooper, L.W., Feder, H.M., Sirenko, B.I., 2006. Ecosystem dynamics of the pacific-influenced northern Bering and Chukchi seas in the Amerasian Arctic. Prog. Oceanogr. 71, 331–361.

Grebmeier, J.M., Moore, S.E., Overland, J.E., Frey, K.E., Gradinger, R., 2010. Biological response to recent Pacific Arctic sea ice retreats. EOS, Trans. American Geophys. Union 18, 161–162.

Harvey, H.R., Sigler, M.F., 2013. An introduction to the Bering Sea Project: volume II. Deep-Sea Res. Pt. II 94, 2–6.

Hewitt, J., Thrush, S., Legendre, P., Funnell, G., Ellis, J., Morrison, M., 2004. Mapping of marine soft-sediment communities: integrated sampling for ecological interpretation. Ecol. Appl. 14, 1203–1216.

Iken, K., Mueter, F., Grebmeier, J., Cooper, L., Danielson, S., Bluhm, B., 2018. Developing an observational design for epibenthos and fish assemblages in the Chukchi Sea. Deep-Sea Res. Pt. II. . https://doi.org/10.1016/j.dsr2.2018.11.005.

Kendall, M., Jensen, O., Alexander, C., Field, D., McFall, G., Bohne, R., Monaco, M., 2005. Benthic Mapping using sonar, video transects, and an innovative approach to accuracy assessments: a characterization of bottom features in the Georgia Bight. J. Coast. Res. 21, 1154–1165.

Kortsch, S., Primicerio, R., Beuchel, F., Renaud, P.E., Rodrigues, J., Lønne, O.J., Gulliksen, B., 2012. Climate-driven regime shifts in Arctic marine benthos. Proc. Natl. Acad. Sci. Unit. States Am. 109, 14052–14057.

Lomas, M.W., Stabeno, P.J., 2014. An introduction to the Bering Sea Project: volume III. Deep-Sea Res. Pt. II 109, 1–4.

Lovvorn, J.R., North, C.A., Grebmeier, J.M., Cooper, L.W., Kolts, J.M., 2018. Sediment organic carbon integrates changing environmental conditions to predict benthic assemblages in shallow Arctic seas. Aquat. Conserv. 28, 861–871.

Lovvorn, J.R., North, C.A., Kolts, J.M., Grebmeier, J.M., Cooper, L.W., Cui, X., 2016. Projecting the effects of climate-driven changes in organic matter supply on benthic food webs in the northern Bering Sea. Mar. Ecol.: Prog. Ser. 548, 11–30.

McGoningle, C., Brown, C., Quinn, R., Grabowski, J., 2009. Evaluation of image-based multibeam sonar backscatter classification for benthic habitat discrimination and mapping at Stanton Banks, UK. Estuar. Coast Shelf Sci. 81, 423–437.

Moore, S.E., Grebmeier, J.M., 2018. The Distributed Biological Observatory: linking physics to biology in the Pacific Arctic region. Arctic 71 (Suppl. l), 1–7.

Mueter, F.J., Weems, J., Farley, E.V., Kuletz, K., Lauth, R.R., Sigler, M.F., 2018. Arctic ecosystem integrated survey final report on distribution of fish, crab, and lower trophic communities in the northeastern Bering Sea and Chukchi sea. US dept. Of the interior, bureau of ocean energy management, Alaska OCS region. OCS Study BOEM 2017-077, pp. 1558.

Perkins, N.R., Foster, S.D., Hill, N.A., Barrett, N.S., 2016. Image subsampling and point scoring approaches for large-scale marine benthic monitoring programs. Estuar. Coast Shelf Sci. 176, 36–46.

Rattray, A., Ierodiaconou, D., Monk, J., Laurenson, L.J.B., Kennedy, P., 2014. Quantification of spatial and thematic uncertainty in the application of underwater video for benthic habitat mapping. Mar. Geodes. 37, 315–336.

Ravelo, A.M., Konar, B., Trefry, J.H., Grebmeier, J.M., 2014. Epibenthic community variability in the northeastern Chukchi Sea. Deep-Sea Res. Pt. II 102, 119–131. https://doi.org/10.1016/j.dsr2.2013.07.017.

Romero-Ramirez, A., Grémare, A., Bernard, G., Pascal, L., Maire, O., Duchêne, J.C., 2016. Development and validation of a video analysis software for marine benthic applications. J. Mar. Syst. 162, 4–17.

Stoker, S.W., 1978. Benthic Invertebrate Macrofauna of the Eastern Continental Shelf of the Bering/Chukchi Seas. Ph.D Thesis, University of Alaska Fairbanks.

Strong, M., Lawton, P., 2004. URCHIN- Manually-deployed geo-referenced video system for underwater reconnaissance and coastal habitat inventory. In: Canadian Technical Report of Fisheries and Aquatic Sciences 2553. Fisheries and Oceans Canada, New Brunswick, Canada.

Van Pelt, T.I., Napp, J.M., Ashjian, C.J., Harvey, H.R., Lomas, M.W., Sigler, M.F., Stabeno, P.J., 2016. An introduction and overview of the Bering Sea Project: volume IV. Deep-Sea Res. Pt. II 134, 3–12.

Wiese, F.K., Wiseman, W.J., Van Pelt, T.I., 2012. Bering Sea linkages. Deep-Sea Res. Pt. II 65–70, 2–5.